

HIGH ENERGY-DENSITY PLASMA DYNAMICS in PLASMA-FILLED ROD-PINCH DIODES*

B.V. Weber[‡], J. P. Apruzese[#], D. Mosher[#], D. G. Phipps, J. W. Schumer, S. J. Stephanakis[#]

*Plasma Physics Division, Naval Research Laboratory
Washington, DC, USA*

Abstract

High energy-density plasma (HEDP) is created using a plasma-filled rod pinch diode (PFRP) [1] on the Gamble II generator. HEDP is produced by a 1-2 MeV, 500 kA electron beam that deposits energy at the end of a tungsten rod. When the rod is tapered to a point, the energy density is estimated to reach 2.4 MJ/cm^3 in about 10 ns, before rapid expansion decreases the energy density.

Recent measurements show that the temperature peaks at about 30 eV at the time of maximum energy density, and that the time-averaged ionization is about +17, similar to MHD model predictions [2]. The plasma mass distribution is inferred from x-ray distribution measurements. The time-dependent mass distribution is used to calculate the mass density and plasma pressure. These measurements indicate the HEDP is strongly coupled ($\Gamma = 35$) with peak pressure (16 Mb) about 7 times greater than $n_e kT$.

I. INTRODUCTION

High Energy Density Plasmas (HEDP), generally defined as plasmas with energy densities greater than 0.1 MJ/cm^3 or pressures greater than 1 Mb, are subjects of current research [3]. One challenge is to produce and diagnose HEDP in the laboratory. This paper reports measurements of HEDP parameters created in tungsten using a Plasma-Filled Rod-Pinch diode (PFRP) [1].

The PFRP is connected to the Gamble II pulsed power generator (2 MV, 0.7 MA, 60 ns with a matched 3-Ohm load) as shown in Fig. 1a. The positive-voltage electrode is terminated in vacuum with a 1 mm diameter tungsten rod. The end of the rod is tapered to a more-or-less sharp point. The rod extends 25 mm through a hole in a flat, grounded cathode plate. Six cable guns inject plasma starting about 1 μs prior to the start of the generator current. Figure 1a is a notional picture of the plasma after the current has increased to about 500 kA in 50 ns, and after being displaced in the axial and radial directions by

$\mathbf{J} \times \mathbf{B}$ forces. When the plasma is swept away, a high-energy ($\sim \text{MeV}$) electron beam connects the plasma to the rod tip. The electron beam heats the tungsten, creating HEDP, and produces bremsstrahlung.

Typical electrical and x-ray waveforms for the PFRP on Gamble II are shown in Fig. 1b. The current waveform (blue line) increases to over 400 kA before the x-ray signal (green line) starts. The voltage (red line) between the cathode disk and the rod is calculated using an upstream voltage monitor, and subtracting $L di/dt$ where L is the inductance between the voltage probe and the cathode plane. The voltage exceeds 1 MV during the rise time (about 10 ns, yellow shaded region) of the x-ray signal and the coupled energy (magenta line) is about 10 kJ in this time interval. The zero time is chosen to be the start of the x-ray signal for synchronizing data from different shots.

Previous modeling [2] assumed the tungsten plasma had a time-dependent Gaussian radial profile and a fixed length of 3.5 mm, consistent with time-integrated x-ray images. A self-similar hydrodynamic expansion model based on Sesame-tabulated equation of state data indicates the maximum energy density is about 2.4 MJ/cm^3 at 10 ns. At this time, the predicted tungsten ionization is +10, $T = 25 \text{ eV}$ and the mass density on axis is close to solid (19 g/cm^3).

II. HEDP DIAGNOSTICS

The diagnostics used to measure the HEDP plasma parameters are described in Fig. 2. Filtered x-ray diodes (XRDs, Fig. 2a) are used to measure the plasma temperature. L-line spectroscopy (Fig. 2b) provides data that determines the time-integrated ionization. An array of 20 pin diodes (Fig. 2c) records x-ray signals behind a thick “rolled edge” to measure the x-ray distribution as a function of time. The x-ray distribution measurements determine the mass density distribution, used to calculate the plasma pressure (independent of temperature and ionization).

* Work supported by the US Office of Naval Research

[‡] email: bruce.weber@nrl.navy.mil

[#] Consultant to NRL through Engility Corp., Chantilly, VA

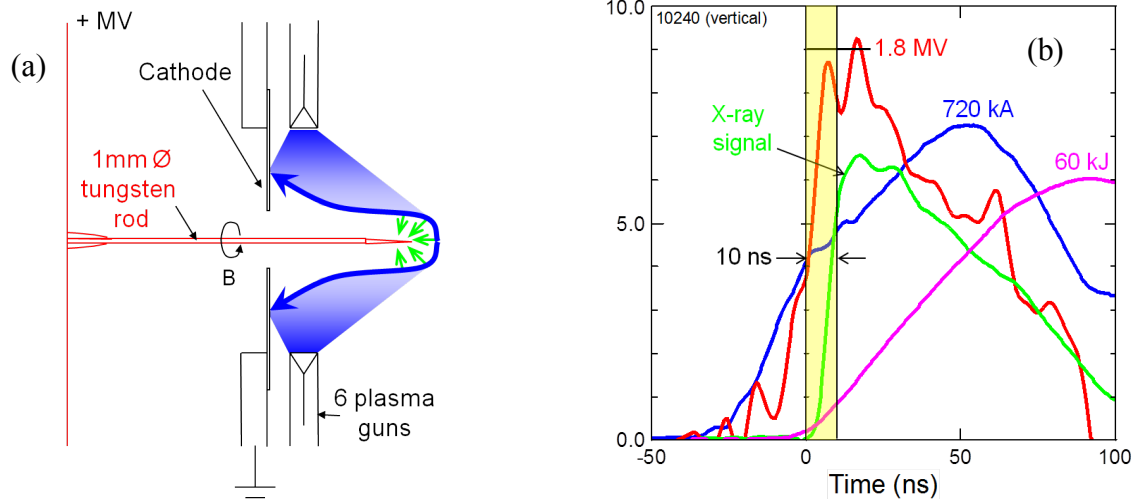


Figure 1. (a) PFRP setup: MeV electrons (green arrows) strike the tip of the tapered tungsten rod, creating an intense x-ray source and high energy density plasma. (b) Electrical and x-ray signals.

A. XRD measurements

The XRD technique in Fig. 2a is a standard method for measuring temperatures in the 10-1000 eV range [4]. Photons from the PFRP pass through a filter before interacting with an aluminum-foil photocathode. Two XRDs with different filters (1.8 μm polycarbonate and 0.8 μm aluminum) have appropriate responses to determine the plasma temperature from the signal ratio. The polycarbonate-filtered XRD response increases monotonically while the aluminum-filtered XRD response decreases monotonically with temperature in the 10-50 eV range. Grids (dotted lines in Fig. 2a) reduce the photon flux and apertures reduce scattered light signals. B fields

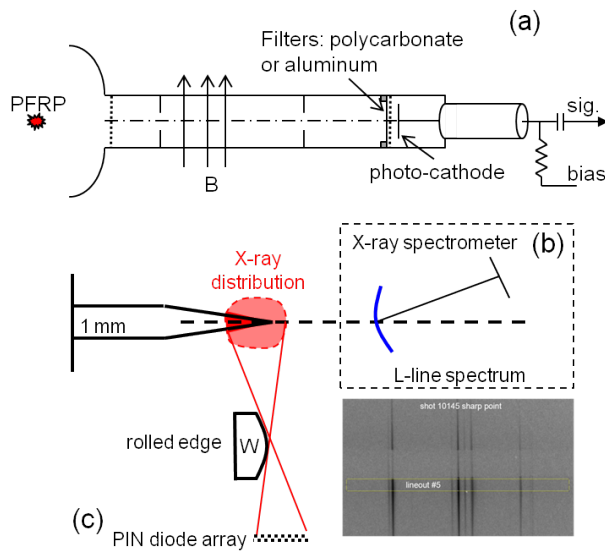


Figure 2. (a) XRD (temperature diagnostic), (b) L-line spectrometer (ionization diagnostic), (c) PIN diode array (x-ray distribution diagnostic).

from permanent magnets deflect charged particles. The distance from the PFRP to the photocathode is adjusted to obtain a desired signal level. On Gamble II, the distances were 1.3 m for the polycarbonate-filtered XRD and 1.9 m for the aluminum-filtered XRD.

The temperature derived from the XRD signal ratio is shown in Fig. 3a for a typical PFRP shot. The XRD signals are very small during the low impedance phase of the PFRP. The XRD signal begins slightly earlier than the hard (bremsstrahlung) x-ray signal. The temperature reaches its peak value, 30 eV, during the rise of the x-ray signal.

B. L-line spectroscopic measurements

A high sensitivity x-ray spectrometer [5] records time-integrated line spectra from the PFRP plasma. The diagnostic and data analysis are described in [6]. A typical spectrum recorded using an image plate is shown in Fig. 2b below the diagram of the spectrometer. The energy range is 8-12 keV, encompassing tungsten's $L\alpha$, $L\beta$ and $L\gamma$ lines. The $L\beta_2$ line (Fig. 3b) is shifted to higher energy by 21 eV, and broadened relative to the other L lines. The energy shift is attributed to an average ionization of +17 and the $L\beta_2$ line shape is attributed to ionization states in the +10 to +28 range that are present at different times during the pulse.

C. X-ray distribution measurements

The rolled edge technique (Fig. 2c) is a standard way to measure radiographic source distributions, usually end-on and time-integrated. The PFRP x-ray source distributions are measured side-on with ~ 1 ns time resolution using an array of 20 pin diodes. The array is aligned either in the axial (parallel to the axis) or vertical (perpendicular to the axis) direction. Each 1×1 mm pin diode is part of a linear strip of 10 diodes. Two parallel

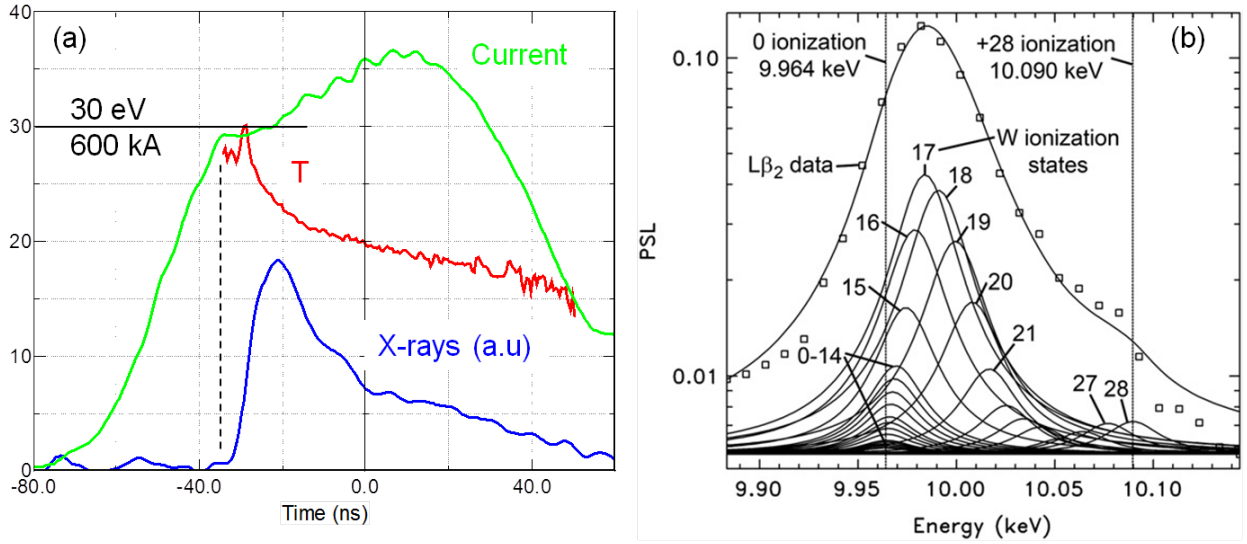


Figure 3. (a) Temperature vs. time (b) $L\beta_2$ line shape (squares, time integrated) is shifted to 20 eV higher energy and broadened by multiple ionization states between +10 and +28 (from Ref. 6).

strips are staggered to make an array of 20 diodes with 0.5 mm between adjacent centers. The pin diodes are cross-calibrated and time-synchronized using data from a flat-field shot without the rolled edge. The magnification $M = (\text{rolled edge} - \text{pin array}) / (\text{rolled edge} - \text{PFRP})$ was 2 for the axial measurements and 3 for the vertical measurements.

At a given time, the signal amplitudes are plotted vs. position (the “edge spread” function). For a Gaussian

source distribution, $\sim \exp(-(r/a)^2)$, the edge spread is an offset error function, $\sim 1 + \text{erf}[(y-y_0)/a]$. Error-function fits to the edge spreads are excellent for the vertical array data and good for the axial array data. The fits give the $1/e$ widths, a_y for the vertical array data and a_z for the axial data.

The resulting vertical and axial, Gaussian x-ray distributions are plotted in Fig. 4 at several times. Above each plot is a visible-light photograph of the rod taken

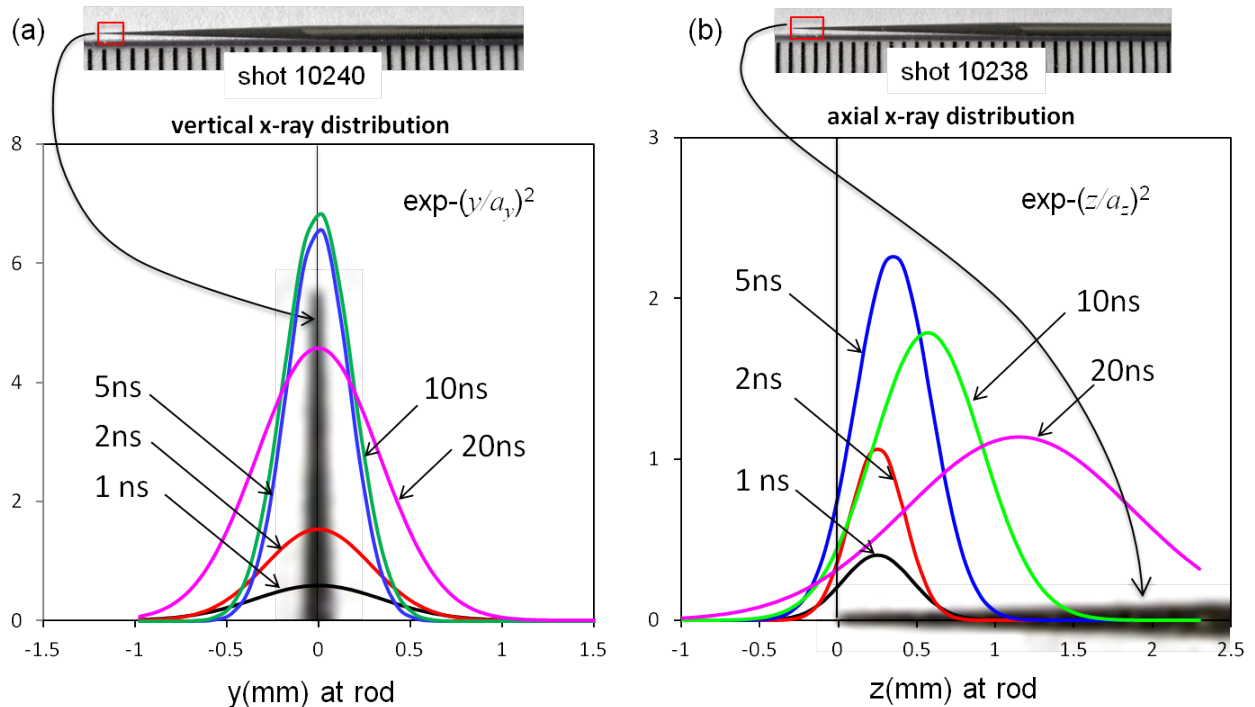


Figure 4. X-ray distributions from (a) vertical pin diode array, (b) axial pin diode array.

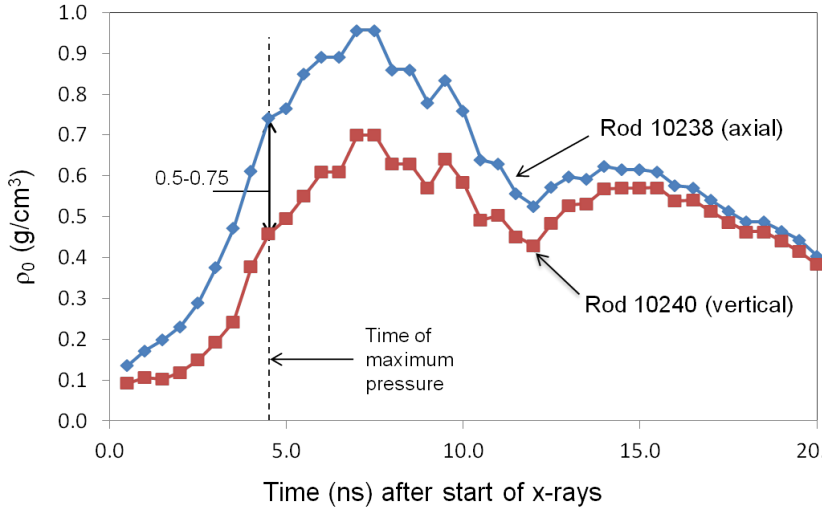


Figure 5. Mass density on axis vs. time, calculated assuming two different rod shapes.

prior to the shot. A blowup of the rod tip is superimposed on each plot to compare with the x-ray distributions. At $t = 1$ ns, the vertical x-ray distribution (Fig. 4a) extends well beyond the original rod boundary implying the tungsten is expanded prior to the start of the x-rays, possibly the result of joule heating by the generator current flowing through the small-radius tip prior to the

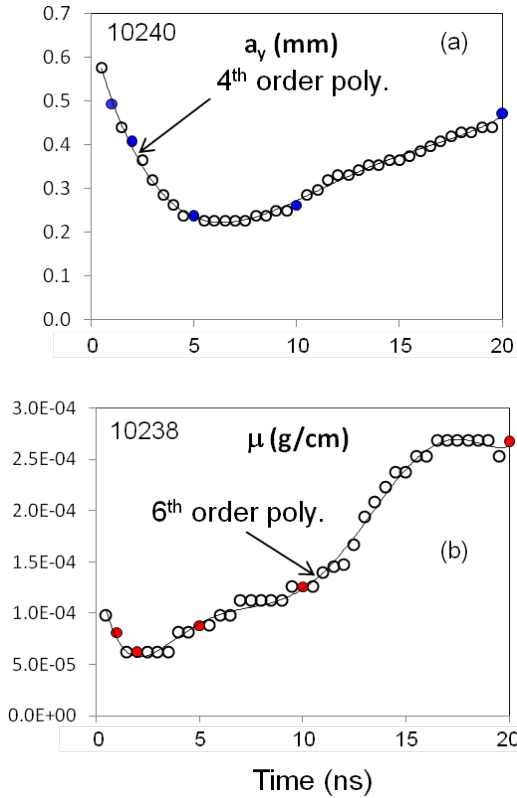


Figure 6. (a) Vertical scale length and (b) mass per unit length as functions on time. Filled symbols are at $t = 1, 2, 5, 10$, and 20 ns, the times plotted in Fig. 4.

formation of the electron beam. From 1-5 ns, the vertical distribution becomes more narrow (a_y decreases). The axial distribution (Fig. 4b) originates near the rod tip, increasing in amplitude from 1-5 ns. From 5-20 ns the axial and vertical scale lengths both increase.

III. DATA ANALYSIS

The tungsten radial mass distribution is assumed to be the same as the measured vertical x-ray distribution. This assumption is valid if the electron energies are high enough so their range is much greater than the plasma thickness, and the plasma is transparent to the x-rays recorded by the pin diodes. Both of these conditions should

be true for the PFRP experiments on Gamble II. The electron range exceeds the $\sim .05$ g/cm² tungsten thickness for energies greater than 0.15 MeV. The pin diodes respond to x-rays that are transmitted through a 13 mm thick plastic vacuum window; half of the pin diode signal is from x-ray energies greater than 300 keV. The tungsten HEDP is highly transparent to these x-rays. The axial x-ray distribution and the *a priori* rod photograph are used to infer the HEDP mass. Together, these measurements are used to calculate the radial mass distribution and the plasma pressure.

A. Mass density

The length of the HEDP is taken to be 1.9 times the axial scale length, a_z . This choice includes 82% of the radiation and discounts the lower-radiation wings of the distribution. The rod photographs (Fig. 4) are used to calculate the initial tungsten mass between the tip and $z = 1.9a_z$. The mass per unit length, μ , is assumed to be this mass divided by $1.9a_z$ for the tungsten HEDP.

The radial mass-density distribution, $\rho(r)$, is derived from the vertical x-ray distribution and μ . Since the vertical distribution is Gaussian, the radial distribution is also Gaussian with the same scale length a_y . The mass distribution is then:

$$\rho(r) = \rho_0 \exp(-r/a_y)^2, \\ \text{where } \rho_0 = \mu/(\pi a_y^2).$$

The density on axis, ρ_0 , for each rod in Fig. 4 is plotted vs. time in Fig. 5. The rod shapes were not identical; the end diameters were 0.55 mm for shot 10240 with the axial array and 0.75 mm for shot 10238 with the vertical array. The peak densities are 0.7 and 0.95 g/cm³ at $t = 7$ ns. (This uncertainty would be eliminated by measuring both x-ray distributions on the same shot.) At the time of maximum pressure (4.5 ns, see below) the density is 0.45-0.75 g/cm³.

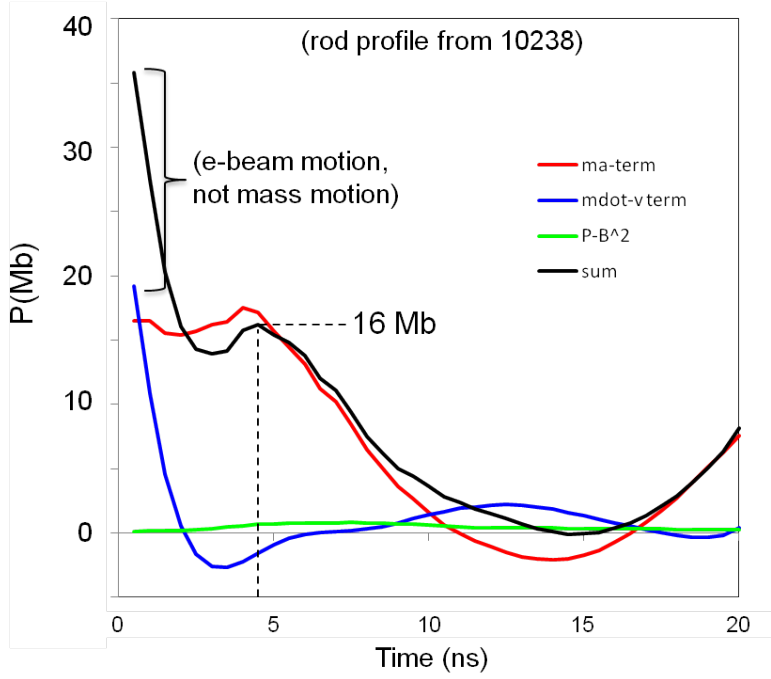


Figure 7. Pressure calculated from mass dynamics. Total pressure (black line) is sum of three terms, mass-acceleration (red), $m \cdot v$ (blue) and magnetic pressure (green).

The ion coulomb coupling parameter, Γ , is the ratio of potential energy to kinetic energy [7]:

$$\Gamma = \frac{\langle PE \rangle}{\langle KE \rangle} = 36 \left(\frac{Z}{6} \right)^2 \left(\frac{A}{12} \right)^{-1/3} \left(\frac{\rho_m}{10^6 \text{ g/cm}^3} \right)^{1/3} \left(\frac{T}{10^7 \text{ K}} \right)^{-1}.$$

Using the measured PFRP parameters: $Z = 17$, $A = 184$, $\rho_m = 0.7$, $T = 30$ eV, gives $\Gamma = 35$, therefore the PFRP plasma is strongly-coupled ($\Gamma > 1$).

B. Plasma pressure

The expansion of the HEDP mass distribution is attributed to its internal pressure. The pressure can be calculated from Newton's second law, written in terms of the measured parameters of the x-ray distributions:

$$P_0 (\text{cgs}) = \frac{1}{2\pi a_y} \left(\mu \frac{d^2 a_y}{dt^2} + \frac{d\mu}{dt} \frac{da_y}{dt} \right) + \frac{I^2(A)}{200\pi a_y^2}.$$

The first term in brackets is the mass-times-acceleration term; the second term is the mass-derivative times velocity. The last term is the maximum magnetic pressure. The time-dependent parameters a_y and μ are plotted in Fig. 6a and b. The measured values (symbols) are fit by polynomial functions that are used to calculate the time-derivatives in the pressure equation.

An example pressure calculation is shown in Fig. 7. The three components in the pressure equation are plotted, with the total pressure indicated by the black line. The initial pressure is high, but this is probably an artifact of electron beam motion instead of mass motion ($d\mu/dt$ and da_y/dt are both negative). For $t = 2$ -10 ns, the pressure is

dominated by the mass-time-acceleration term. At $t = 4.5$ ns there is a local maximum in the pressure of 16 Mb. The pressure is calculated using the mass per unit length for the rod with the larger tip diameter. The pressure is about 9 Mb when the other rod tip is used in the calculation. This large uncertainty could be eliminated by measuring both x-ray distributions during the same shot.

This calculated pressure is compared with $n_e kT$, using the mass density at $t = 4.5$ ns in Fig. 5. The density range at this time is 0.45 - 0.75 g/cm^3 , or $n_i = 1.5$ - $2.5 \times 10^{21} \text{ cm}^{-3}$. Assuming $(1+Z) = 20$, $n_e = (1+Z) n_i = 3$ - $5 \times 10^{22} \text{ cm}^{-3}$ and $n_e kT = 1.4$ - 2.4 Mb . This pressure calculated from the expansion of the plasma is higher than these values by about a factor of 7. The reason for the higher pressure is the strong coupling between plasma ions, and the inability of the plasma electrons to completely screen the ion-ion coulomb forces. The number of electrons in a Debye sphere is approximately 1.6, so normal screening approximations are not valid.

IV. SUMMARY

This paper reports measurements of HEDP parameters created at the tip of a tapered tungsten rod in a PFRP diode. The plasma parameters are in the Warm Dense Matter (WDM) regime: $T = 30$ eV, $\rho = 0.7 \text{ g/cm}^3$, $Z = 17$, and $P = 16 \text{ Mb}$. The plasma ions are strongly coupled, with $\Gamma = 35$. The pressure is calculated from the measured plasma expansion, independent of temperature and ionization, and is found to exceed nkT by about a factor of 7. This HEDP is produced by a "standard" pulsed power generator, representing a new way to produce WDM in the laboratory.

The HEDP parameters presented here are the result of measurements made during different shots. All the diagnostics could be implemented on the same shot in future experiments to eliminate uncertainties from shot-to-shot variations (due to different rod dimensions, for example). The spectroscopic diagnostic could be made time-resolved using an x-ray streak or framing camera. The x-ray distribution measurements could be improved, with precise alignment between pin diodes and the rod tip, and with two arrays and two rolled edges. Two-dimensional x-ray imaging [8] would be useful for comparison with 2D models. An improved diagnostic suite could then be used to explore the dependence of the HEDP parameters on variations in the diameter of the rod tip or the pulsed power parameters.

V. REFERENCES

- [1] B.V. Weber, R. J. Commisso, G. Cooperstein, D.D. Hinshelwood, D. Mosher, P. F. Ottinger, D. M. Ponce, J.W. Schumer, S.J. Stephanakis, S. B. Strasburg, S.B. Swanekamp, and F.C. Young, "Ultra-High Electron Beam Power and Energy Densities Using a Plasma-Filled Rod-Pinch Diode," *Phys. Plasmas*, vol. 11, pp. 2916-2927, May 2004.
- [2] D. Mosher, J.W. Schumer, B.V. Weber, and D. Ponce, "Electrode-Expansion MHD in a Plasma-Filled Rod Pinch," in *Proc. 14th IEEE Int. Pulsed Power Conference*, (Dallas, TX, June 2003), p. 503.
- [3] National Research Council, *Plasma Science: Advancing Knowledge in the National Interest*. Washington, DC: The National Academies Press, 2007.
- [4] J.R. Kearns and D.J. Johnson, "Study of an Electron-Beam Discharge into a Vacuum Diode with Polyethylene Anode," *J. Appl. Phys.*, vol. 45, pp. 5225-5228, Dec. 1974.
- [5] J.F. Seely, R. Doron, A. Bar-Shalom, L.T. Hudson, C. Stroeckl, J.F. Seely, U. Feldman, C. Brown, N. Pereira, L. Hudson, J. Glover, E. Silver, "Transmission Crystal X-Ray Spectrometer Covering the 6 keV-18 keV Energy Range with $E/\Delta E = 1800$ Instrumental Resolving Power," *Rev. Sci. Instrum.*, vol. 83, pp. 10E112-1 to 10E112-3, 2012.
- [6] J.F. Seely, B.V. Weber, D.G. Phipps, N.R. Pereira, D. Mosher, K. Slabkowska, M. Polasik, J. Starosta, J. Rzakiewicz, S. Hansen, U. Feldman, L.T. Hudson, J.W. Schumer, "Tungsten L Transition Line Shapes and Energy Shifts Resulting From Ionization in Warm Dense Matter," *High Energy Density Physics*, vol. 9, pp. 354-362, March 2013.
- [7] S. Ichimaru, H. Iyetomi and S. Tanaka, "Statistical Physics of Dense Plasmas: Thermodynamics, Transport Coefficients and Dynamic Correlations," *Phys. Rep.* 149, Nos. 2 & 3, pp. 91-205, 1987.
- [8] G. Barnea, "Penumbral Imaging Made Easy," *Rev. Sci. Instrum.*, vol. 65, pp. 1949-1953, June 1994.